

Shell-dependent electroluminescence from colloidal CdSe quantum dots in multilayer light-emitting diodes

Pengtao Jing, Jinju Zheng, Qinghui Zeng, Youlin Zhang, Xiaomin Liu et al.

Citation: *J. Appl. Phys.* **105**, 044313 (2009); doi: 10.1063/1.3079475

View online: <http://dx.doi.org/10.1063/1.3079475>

View Table of Contents: <http://jap.aip.org/resource/1/JAPIAU/v105/i4>

Published by the [American Institute of Physics](#).

Related Articles

Nanoscale fluorescence imaging with quantum dot near-field electroluminescence

Appl. Phys. Lett. **101**, 043118 (2012)

Blue light emitting diode internal and injection efficiency

AIP Advances **2**, 032117 (2012)

Enhancement of hole injection and electroluminescence characteristics by a rubbing-induced lying orientation of alpha-sexithiophene

J. Appl. Phys. **112**, 024503 (2012)

Study of field driven electroluminescence in colloidal quantum dot solids

J. Appl. Phys. **111**, 113701 (2012)

Indium incorporation and emission properties of nonpolar and semipolar InGaN quantum wells

Appl. Phys. Lett. **100**, 201108 (2012)

Additional information on J. Appl. Phys.

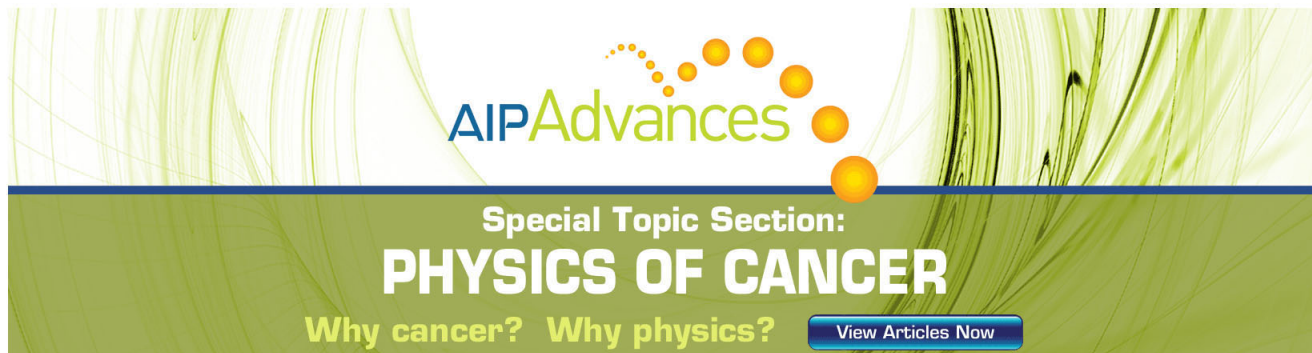
Journal Homepage: <http://jap.aip.org/>

Journal Information: http://jap.aip.org/about/about_the_journal

Top downloads: http://jap.aip.org/features/most_downloaded

Information for Authors: <http://jap.aip.org/authors>

ADVERTISEMENT



The advertisement banner features a green background with abstract, flowing lines. At the top, the text "AIPAdvances" is displayed in a stylized font, with "AIP" in blue and "Advances" in green. Below this, the text "Special Topic Section:" is written in white, followed by "PHYSICS OF CANCER" in large, bold, white capital letters. At the bottom, the text "Why cancer? Why physics?" is written in yellow, and a blue button with the text "View Articles Now" is located on the right side.

Shell-dependent electroluminescence from colloidal CdSe quantum dots in multilayer light-emitting diodes

Pengtao Jing,^{1,2} Jinju Zheng,^{1,2} Qinghui Zeng,^{1,2} Youlin Zhang,^{1,2} Xiaomin Liu,¹ Xueyan Liu,¹ Xianggui Kong,¹ and Jialong Zhao^{1,a)}

¹Key Laboratory of Excited State Processes, Changchun Institute of Optics, Fine Mechanics and Physics, Chinese Academy of Sciences, 3888 Eastern South Lake Road, Changchun 130033, China

²Graduate School of Chinese Academy of Sciences, Beijing 100039, China

(Received 17 December 2008; accepted 2 January 2009; published online 27 February 2009)

We report electroluminescence (EL) of colloidal CdSe/CdS, CdSe/ZnS, and CdSe/CdS/CdZnS/ZnS core/shell quantum dots (QDs) in multilayer light-emitting diodes (LEDs) fabricated by spin coating a near monolayer of the core/shell QDs on cross-linkable hole transporting layers. It is found that CdSe/CdS QD-LEDs exhibit a faster decrease in EL quantum efficiency ($\sim 2\%$ at a brightness of 100 cd/m^2) with increasing current density and lower maximum brightness than those of CdSe/ZnS QD-LEDs. A more significant redshift and spectral broadening of the EL observed in CdSe core/shell QDs with a CdS or CdS/CdZnS/ZnS shell than with a ZnS shell indicate that the electron wave function can penetrate into the shell under electric field. The difference in device performance and EL spectra results from conduction band offsets between the CdSe cores and CdS or ZnS shells, suggesting the existence of the exciton ionization in the QD-LEDs. © 2009 American Institute of Physics. [DOI: 10.1063/1.3079475]

I. INTRODUCTION

Semiconductor quantum dots (QDs) as the inorganic chromophores have been used as recombination centers in light-emitting diodes (LEDs) to precisely control the emission color by changing the size or composition of QDs.^{1–18} Recently, bright color-saturated emissions were demonstrated in QD-LEDs by use of monodisperse QDs and a multilayer device configuration, making them promising for the next generation display and lighting.^{3,10–18} The performance of QD-LEDs including the external quantum efficiency (QE) and brightness has been rapidly improved by using high quality QDs during the past ten years. However, the early QD-LEDs showed a relatively low external QE (below 0.01%) and impure electroluminescence (EL) from both the QDs and organic host materials mainly due to the use of single- or bilayer device structures and the imbalance of carrier injection into QDs.^{1,2} A major breakthrough in device performance with an external QE of 0.5% at a brightness of 190 cd/m^2 was realized in 2002 when a QD-LED structure that incorporated just a single monolayer of CdSe/ZnS core/shell QDs sandwiched between organic hole-transport layer (HTL) and electron-transport layer was demonstrated.³ With subsequent refinement, a maximum external QE of about 2.0% and luminous efficiency of more than 2.0 cd/A could be reached.^{11,13,14,17}

The key to further optimize the performance of QD-LEDs seems to be a detailed understanding of the EL mechanism and the resulting design of core/shell QDs with better structures. The EL from a single monolayer of CdSe/ZnS core/shell QDs within a multilayer LED was qualitatively explained by exciton generation in the QDs through either

direct charge injection or exciton energy transfer from the organic molecules.³ In contrast, the EL from the QD-LEDs with a multilayer of CdSe/ZnS QDs was considered to only come from exciton generation through free carrier injection into QDs.¹⁴ The photoluminescence (PL) QE and photostability of the CdSe core QDs are significantly improved by the growth of CdS and ZnS shells,^{19,20} whereas the contradictory results were reported on improved EL efficiency in devices with CdSe/CdS QDs, in comparison to CdSe/ZnS particles.^{5,6} More importantly, PL quantum yield (QY) of CdSe QDs was significantly improved up to 85% by using a CdS/CdZnS/ZnS multishell.^{21,22} To date, the shell effect on device performance has not been understood yet.

In this work, we study the EL of CdSe core/shell QDs in multilayer QD-LEDs with a single monolayer (ML) of the QDs onto cross-linked double HTLs, which consist of a layer of two connecting diamine molecules or [*N,N'*-bis(1-naphthyl)-*N,N'*-diphenyl-1,1'-biphenyl-4,4'-diamine] functionalized with two styryl groups (2-TPD) or 2-NPD (Ref. 23) and a layer of 4,4',4''-tri(*N*-carbazolyl)triphenylamine bis(vinylbenzyl ether) (TCTA-VB). We examine the change in the EL performance of the QD-LEDs and spectra of the QDs under electric fields by varying the shell materials and thicknesses to understand the EL mechanism in QD-LEDs. We demonstrate lower performance and larger redshift and linewidth broadening of EL in the devices with CdSe/CdS QDs than CdSe/ZnS QDs, suggesting the extension of the exciton wave function into the shell under electric field and the ionization of excitons in core/shell QDs.

II. EXPERIMENT

The CdSe QDs were synthesized using the successive ion layer adsorption and reaction method.²¹ The PL QE and

^{a)}Author to whom correspondence should be addressed. Electronic mail: zhaojl@ciomp.ac.cn.

photostability of the CdSe QDs are significantly improved by the growth of CdS, CdZnS, and ZnS shells. The thicknesses of all the CdS, CdZnS, and ZnS shells were varied from 1 to 6 MLs. For use in the QD-LEDs, the as-prepared QDs were further purified to remove excess ligands and synthetic by-products. Postsynthesis, all QD samples were twice washed by dissolution in chloroform and subsequent precipitation with acetone followed by drying under N_2 . The removal of organic ligands from the core/shell QDs causes a drop of the QY by about 30%.

The fabrication of the multilayer QD-LEDs is described as follows: the 20 nm thick cross-linkable HTL, 2-TPD, was first spin coated onto a plasma-cleaned indium tin oxide (ITO) slide and then thermally cross-linked by heating to 180 °C for 30 min.²³ Then 20 nm TCTA-VB was spin coated on top of the TPD-VB layer and thermally cross-linked at 180 °C for 30 min to impart solvent resistance. We use the 2-TPD layer instead of polystyrene-*N,N'*-diphenyl-*N,N'*-bis(4-*n*-butylphenyl)-(1,1'-biphenyl)-4,4'-diamine-perfluorocyclobutane (PS-TPD-PFCB) polymer in a previous QD-LED paper¹² because 2-TPD can be cross-linked at lower temperatures and has a better hole-transport ability. Typical root mean square (rms) surface roughness of double HTLs, 2-TPD(20 nm)/TCTA-VB(20 nm), was estimated to about 1.2 nm. A near monolayer of the CdSe core/shell QDs was spin coated from a chloroform solution with an optical density of 0.5–2.0 at the first excitonic absorption maximum of QDs at a spin speed of 1500 rpm. Following deposition of the QD layer, 40 nm electron-transport layer, 1,3,5-tris(*N*-phenylbenzimidazol-2-yl)benzene (TPBI), was deposited by thermal evaporation. The devices were then completed by thermal evaporation of the back electrode [CsF(1 nm)/Al(120 nm)] through a shadow mask. Each device pixel had an active area of $\pi \times 1^2$ mm². Current-voltage characteristics of the QD-LEDs were measured on a Hewlett Packard 4155B semiconductor parameter analyzer. The EL emission power was measured using a Newport 2835-C multifunction optical meter. EL spectra were recorded with an Oriel InstaSpec IV charge-coupled device camera. Photometric units (cd/m²) were calculated from the forward output power and the EL spectra of the devices, assuming Lambertian distribution of the EL emission. All device measurements were performed under ambient conditions.

III. RESULTS AND DISCUSSION

The surface morphology of the cross-linked HTLs and a near monolayer of CdSe/CdS QDs on HTLs are shown in Fig. 1. As seen in Fig. 1(a), the surface of the cross-linked single HTL, 2-TPD, is very smooth, with a rms surface roughness <0.81 nm. Further the rms surface roughnesses of double HTLs, 2-TPD(20 nm)/TCTA-VB(20 nm) or 2-NPD(20 nm)/TCTA-VB(20 nm), used to improve the device performance¹² were estimated to about 1.22 and 1.31 nm, respectively, as shown in Figs. 1(b) and 1(c). Typically, the surface of a near monolayer of CdSe/CdS QDs is very uniform and smooth, with rms surface roughness <0.82 nm as shown in Fig. 1(d). We use the 2-TPD or 2-NPD layer instead of PS-TPD-PFCB polymer in previous QD-LED

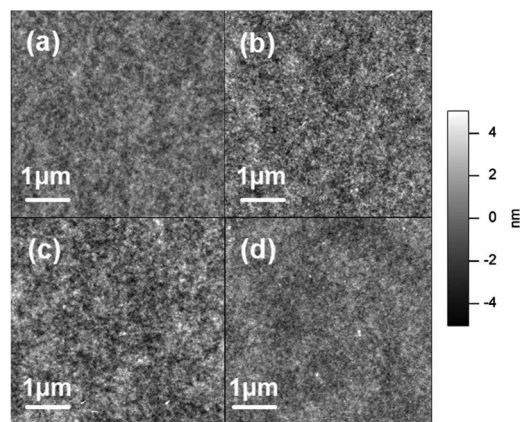


FIG. 1. Atomic force microscopy images of HTLs and a CdSe/CdS QD layer. The images from (a) to (d) represent the surface morphology of ITO/2-TPD (40 nm) (a), ITO/2-TPD(20 nm)/TCTA-VB(20 nm) (b), ITO/2-NPD(20 nm)/TCTA-VB(20 nm) (c), and a near monolayer of CdSe/CdS QDs on ITO/2-TPD(20 nm)/TCTA-VB(20 nm) (d).

paper¹² because 2-TPD or 2-NPD can be cross-linked at lower temperatures and has better ability to transport hole to QDs.²³ Therefore, the high quality QD-LED with a QD layer of controlled thickness can be simply achieved by spin-coating colloidal QDs from organic solution onto the solvent-resistant HTLs and allows one to study the effect of shells on the EL of QDs.

Figure 2 shows single color EL spectra from a near monolayer of CdSe/CdS(3 ML), CdSe/ZnS(3 ML), CdSe/CdS(6 ML), and CdSe/CdS(3 ML)/CdZnS(1 ML)/ZnS(2 ML) core/shell QDs in multilayer QD-LEDs with double HTLs (2-TPD/TCTA-VB) at various biases from 6 to 18 V, respectively. The diameters of the QDs were estimated to be 5.7, 5.8, 7.4, and 8.1 nm. The wavelengths and full widths at half maximum of the EL peaks at 6 V are 596, 575, 611, and 623 nm and 27, 34, 35, and 36 nm, respectively. As seen in Fig. 2(a), the EL peak shifts to the red with increasing for-

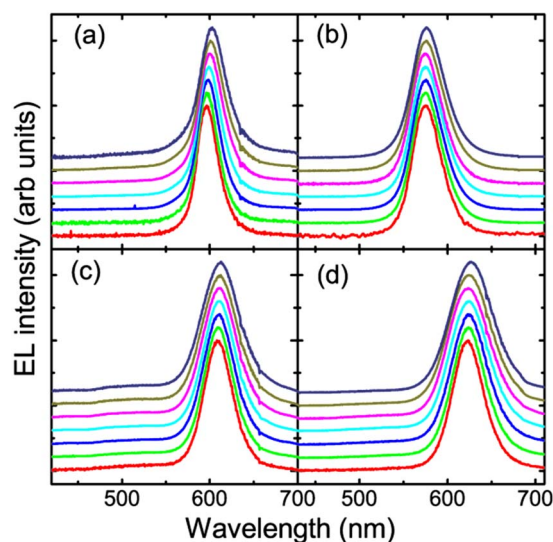


FIG. 2. (Color online) EL spectra of QD-LEDs with CdSe/CdS(3 ML) (a), CdSe/CdS(6 ML) (b), CdSe/ZnS(3 ML) (c), and CdSe/CdS(3 ML)/CdZnS(1 ML)/ZnS(2 ML) QDs (d) at various biases from 6 to 18 V (from bottom to top).

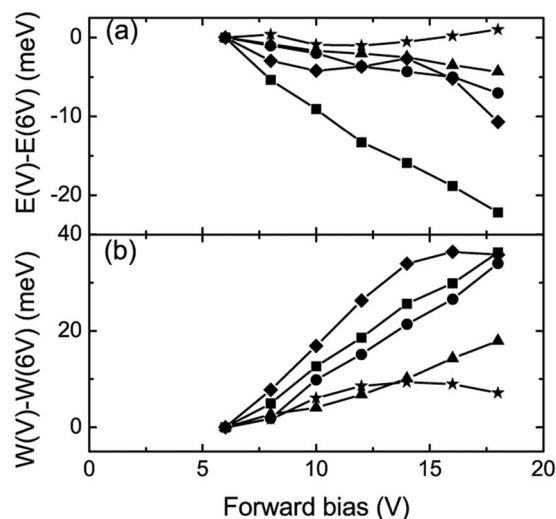


FIG. 3. Shift of peak energy (a) and the change in the linewidth (b) of the EL for QD-LEDs with the CdSe/CdS(3 ML) (squares), CdSe/ZnS(3 ML) (triangles), CdSe/CdS(6 ML) (cycles) core/shell, and CdSe/CdS(3 ML)/CdZnS(1 ML)/ZnS(2 ML) multishell QDs (diamonds) at various forward biases. In comparison, the data from CdSe core QDs are plotted by stars in the figure.

ward bias, resulting in a significant linewidth broadening of the EL in the CdSe/CdS(3 ML) QDs. Similarly, the redshift and linewidth broadening of the EL were demonstrated in CdSe/ZnS(3 ML), CdSe/CdS(6 ML), and CdSe/CdS(3 ML)/CdZnS(1 ML)/ZnS(2 ML) core/shell QDs. The redshift of EL peak with respect to the PL peak was attributed to Förster energy transfer² and a quantum confined Stark effect.^{9,12,24–26} In comparison, the pure EL spectra were obtained from CdSe core QDs in the QD-LEDs with a single HTL (PS-TPD-PFCB). A small redshift (smaller than 2 nm) and linewidth broadening of the EL were observed in these CdSe core QDs under forward bias from 8.0 to 18.0 V. In addition, it was noted that the EL peak shifted to the blue under higher voltage when the QD-LEDs worked for a long time because the core QDs were easily subjected to photo-oxidation.

The voltage dependence of the EL peak energy and linewidth for the CdSe core/shell QDs is shown in Fig. 3. There appears more significant redshift and larger linewidth broadening of EL peak in CdSe/CdS(3 ML) QDs than in CdSe/ZnS(3 ML) ones perhaps due to varied conduction band offsets of 0.2 and 0.9 eV.^{3,5,6} In the QD-LEDs, the electric field can give rise to a tilting of the electronic barriers between CdSe core and the shell and thus lead to a deformation of the carrier wave function; whereas the hole is confined in the core of the particle, the electron wave function can penetrate into the shell, causing a larger spectral redshift and linewidth broadening of EL peaks for CdSe/CdS QDs than for CdSe/ZnS QDs.^{24–26} The electric field-induced PL quenching was observed in CdSe/ZnS QDs recently due to the ionization of excitons.^{27,28} Therefore, the drop in device efficiency with increasing current density should be in part associated with ionization of excitons in the QDs and resulting imbalance of carriers in the QDs. Furthermore, it is found that the significant spectral broadening of EL occurs in CdSe/CdS/CdZnS/ZnS core/multishell QDs as seen in Fig. 3(b). This means that electrons can be delocalized into a CdS shell from a

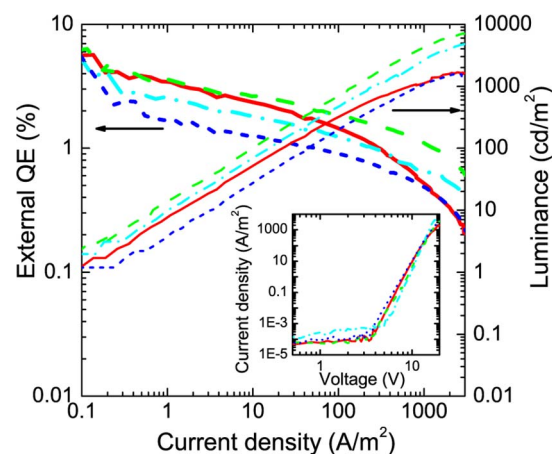


FIG. 4. (Color online) External QE (thick lines) and luminance (thin lines) as a function of current density for CdSe/CdS(3 ML) (solid/red lines), CdSe/ZnS(3 ML) (dashed/green lines), CdSe/CdS(6 ML) (short-dashed/blue lines), and CdSe/CdS(3 ML)/CdZnS(1 ML)/ZnS(2 ML) core/shell QDs (dash-dotted/cyan lines) on double HTLs. Dependence of current density on forward bias for the QD-LEDs is shown in the inset of the figure.

CdSe core under electric field. However, they are still confined inside the CdSe/CdS/CdZnS/ZnS core/shell QDs with a higher barrier of a ZnS shell, resulting in higher external QE and the maximum brightness of the devices at a high forward bias. Therefore, the use of multishells and adjustment of the shell thickness allow one to control the ionization of excitons in the QDs to improve the external QE.

Figure 4 shows the external QE and luminance as a function of current density for the CdSe QD-LEDs with CdSe/CdS(3 ML), CdSe/ZnS(3 ML), CdSe/CdS(6 ML), and CdSe/CdS(3 ML)/CdZnS(1 ML)/ZnS(2 ML). The external QEs of these devices were determined to be 2.1%, 2.6%, 1.1%, and 1.6% at a brightness of 100 cd/m², while the PL QYs were estimated to be 63%, 40%, 47%, and 60% for the core/shell QDs. Further, the brightness increases with current density and saturates at 1660, 7480, 1620, and 4810 cd/m² at 3000 A/m². The dependence of the current density on the forward bias for the QD-LEDs is also shown in the inset of Fig. 4. The current density changes almost linearly with increasing forward bias at below 3 V and rapidly increases above 3 V, consistent with the observation of Coe *et al.*³ As is known the device efficiency depends not only on the PL QY, band gap, and confinement barrier height of QDs but also on the QD layer properties including the number of QDs, the morphology, and the thickness of QD layer, resulting in different injection of electrons and holes.^{3,11,12,14,17} Therefore, we can only pay attention to the difference in the dependence of device efficiency on the current density. As seen in Fig. 4, the external QEs of CdSe/CdS(3 ML) and CdSe/ZnS(3 ML)-based QD-LEDs drop markedly to 0.2% and 0.6% at 3000 cd/m², respectively, from about 2% at 100 cd/m². The corresponding maximum brightness is 1660 and 7480 cd/m², respectively. The faster drop in the device efficiency with increasing current density and more significant saturation in brightness at high electric fields were clearly observed in LEDs incorporating CdS shell coated QDs than those of ZnS- and CdS/CdZnS/ZnS-shelled QD-based LEDs as shown in Fig. 4. Therefore, we confirm a

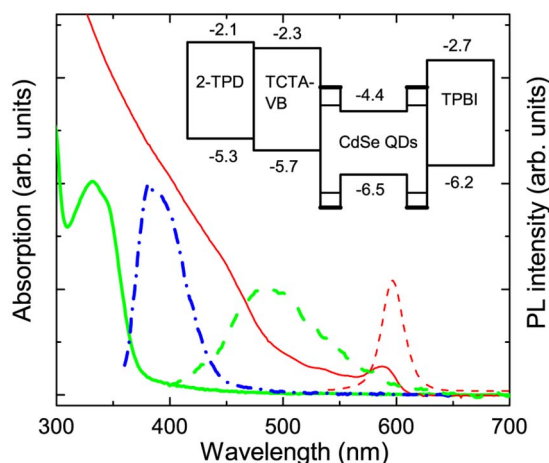


FIG. 5. (Color online) Absorption (solid lines) and PL (dashed lines) spectra of CdSe/CdS(3 ML) QDs (thin/red lines) and TCTA-VB (thick/green lines). The PL spectrum of small molecule TCTA is also shown by a dash-dotted blue line. Energy band diagram for the QD-LEDs is shown in the inset of the figure. The electron affinities and ionization energies of 2-TPD, TCTA-VB, TPBI, and CdSe QDs are taken from Refs. 3, 5, 6, 11, 12, 14, and 17. Conduction and valence band positions for the QDs with CdS and ZnS shells are labeled with thin and thick lines in the inset.

significant difference in the dependence of device efficiency on current density in the CdS and ZnS-shelled QD-LEDs. As a result, the difference cannot be simply attributed to the degradation of QDs or devices because we could not observe the irreversible spectral shift of the EL in core/shell QDs due to the photo-oxidation. This suggests that the mechanism responsible for the drop in device efficiency with increasing current density and the saturation of the brightness at higher electric field is intrinsic to the core/shell QDs and the devices, which may be in part related to the ionization of excitons in QDs. The ionization of exciton means that electron or hole tunnels outside the QDs in the presence of electric field, which should lead to the charging of QDs and resulting decrease of EL QE.^{27,28} Further, it is found that the device efficiency of the CdSe QD-LEDs at 100 cd/m² shows a weak dependence on the shell thickness when the shell thickness of the QDs was varied from 3 to 6 MLs for the CdS shell or from a 3 ML ZnS shell to a 6 ML CdS(3 ML)/CdZnS(1 ML)/ZnS(2 ML) shell.

We hypothesize that the good performance of the QD-LED results from the control of electron and hole injection into QDs by a monoshell or a multishell with optimized surface barriers. The diagram of energy band structure alignment of QDs with respect to the electron energy levels of the hole and electron transporting layers is shown in Fig. 5. We know that the electron injection barrier is nonexistent in the structures while the energy barrier to hole injection is markedly different for CdS and ZnS shells based on the bulk band structure and electron/hole effective mass of the QD materials.^{3,17} As seen in Fig. 5, the hole injection barrier for a ZnS shell is higher than that for a CdS shell. The external QE of the QD-LEDs should be related to the barrier height. In this experiment, we have found that the external QE of CdSe/ZnS QD-LEDs was improved through the use of double HTLs, 2-TPD(20 nm)/TCTA-VB(20 nm) instead of a single HTL, 2-TPD(40 nm), by a factor of about 2. We ex-

pect that the device performance will be improved by decreasing the valence band offset to increase hole injection into QDs.

Resonant exciton energy transfer from TPD and Alq₃ to QDs was considered to contribute to the high QE of the devices due to the spectral overlap between TPD and Alq₃ PL and QD absorption.^{3,11,17} However, the PL of the cross-linked HTLs such as TCTA-VB and 2-TPD near the band edge was completely quenched after a curing process, while a weak and broad PL band peaked at a wavelength of 500 nm was observed like PS-TPD-PFCB, as seen in Fig. 5.²⁹ This means that the Förster exciton energy transfer rate from TCTA-VB or 2-TPD to QDs is expected to be very low. On the other hand, the energy transfer rate for CdSe core(3.6 nm)/CdS shell(6 ML:2.1 nm)/TOPO(1 nm) is less than one-fifth of that for CdSe core(3.6 nm)/CdS shell(3 ML:1.0 nm) based on an estimation from the Förster energy transfer theory.³⁰ As a result, the exciton energy transfer seems to be not responsible for the EL mechanism of the QD-LEDs fabricated by depositing QD layers on the thermally cross-linked HTLs.

IV. CONCLUSIONS

In summary, we have studied EL and device performance of CdSe core CdS, ZnS, and CdS/CdZnS/CdS shell QD-based LEDs and demonstrated a significant difference in the dependence of device performance on current density in the LEDs. The observation of the significant difference in the redshift and linewidth broadening of the EL from the CdSe QDs with various shell structures suggests that the electric field-induced ionization of excitons in the QD-LEDs is dependent on the shell structure. Therefore, the performance of the CdSe QD-LEDs is expected to be further improved by optimizing the shell material and thickness for controlling electrons and holes into QDs and preventing the ionization of excitons in QDs under electric field.

ACKNOWLEDGMENTS

This work was supported by the program of CAS Hundred Talents, NSF of China (Grant Nos. 10874179, 10674132, and 60771051) and the National High Technology Development Program (Grant No. 2006AA03Z335). J.Z. gratefully acknowledges Prof. Alex K.-Y. Jen and Prof. David S. Ginger for their helpful discussion and Dr. Yen-Ju Cheng, Dr. Yanqing Tian, and Dr. Yong Zhang for their help in the preparation of the QD-LEDs.

¹V. L. Colvin, M. C. Schlamp, and A. P. Alivisatos, *Nature (London)* **370**, 354 (1994).

²B. O. Dabbousi, M. G. Bawendi, O. Onitsuka, and M. F. Rubner, *Appl. Phys. Lett.* **66**, 1316 (1995).

³S. Coe, W. K. Woo, M. Bawendi, and V. Bulovic, *Nature (London)* **420**, 800 (2002).

⁴N. Tessler, V. Medvedev, M. Kazes, S. Kan, and U. Banin, *Science* **295**, 1506 (2002).

⁵M. C. Schlamp, X. G. Peng, and A. P. Alivisatos, *J. Appl. Phys.* **82**, 5837 (1997).

⁶H. Mattoussi, L. H. Radzilowski, B. O. Dabbousi, E. L. Thomas, M. G. Bawendi, and M. F. Rubner, *J. Appl. Phys.* **83**, 7965 (1998).

⁷M. Y. Gao, C. Lesser, S. Kirstein, H. Mohwald, A. L. Rogach, and H. Weller, *J. Appl. Phys.* **87**, 2297 (2000).

- ⁸S. Coe-Sullivan, W. K. Woo, J. S. Steckel, M. Bawendi, and V. Bulovic, *Org. Electron.* **4**, 123 (2003).
- ⁹J. L. Zhao, J. Y. Zhang, C. Y. Jiang, J. Bohnenberger, T. Basche, and A. Mews, *J. Appl. Phys.* **96**, 3206 (2004).
- ¹⁰J. S. Steckel, J. P. Zimmer, S. Coe-Sullivan, N. E. Stott, V. Bulovic, and M. G. Bawendi, *Angew. Chem., Int. Ed.* **43**, 2154 (2004).
- ¹¹S. Coe-Sullivan, J. S. Steckel, W. K. Woo, M. G. Bawendi, and V. Bulovic, *Adv. Funct. Mater.* **15**, 1117 (2005).
- ¹²J. L. Zhao, J. A. Bardecker, A. M. Munro, M. S. Liu, Y. H. Niu, I. K. Ding, J. D. Luo, B. Q. Chen, A. K.-Y. Jen, and D. S. Ginger, *Nano Lett.* **6**, 463 (2006).
- ¹³Y. H. Niu, A. M. Munro, Y. J. Cheng, Y. Q. Tian, M. S. Liu, J. L. Zhao, J. A. Bardecker, I. J. Plante, D. S. Ginger, and A. K.-Y. Jen, *Adv. Mater. (Weinheim, Ger.)* **19**, 3371 (2007).
- ¹⁴Q. J. Sun, Y. A. Wang, S. L. Li, D. Y. Wang, T. Zhu, J. Xu, C. H. Yang, and Y. F. Li, *Nat. Photonics* **1**, 717 (2007).
- ¹⁵J. S. Steckel, P. Snee, S. Coe-Sullivan, J. P. Zimmer, J. E. Halpert, P. Anikeeva, L.-A. Kim, V. Bulovic, and M. G. Bawendi, *Angew. Chem., Int. Ed.* **45**, 5796 (2006).
- ¹⁶Y. Q. Li, A. Rizzo, R. Cingolani, and G. Gigli, *Adv. Mater. (Weinheim, Ger.)* **18**, 2545 (2006).
- ¹⁷P. O. Anikeeva, J. E. Halpert, M. G. Bawendi, and V. Bulovic, *Nano Lett.* **7**, 2196 (2007).
- ¹⁸Z. Tan, F. Zhang, T. Zhu, J. Xu, A. Y. Wang, J. D. Dixon, L. Li, Q. Zhang, S. E. Mohny, and J. Ruzyllo, *Nano Lett.* **7**, 3803 (2007).
- ¹⁹M. A. Hines and P. Guyot-Sionnest, *J. Phys. Chem.* **100**, 468 (1996).
- ²⁰B. O. Dabbousi, J. Rodriguez-Viejo, F. V. Mikulec, J. R. Heine, H. Mattoussi, R. Ober, K. F. Jensen, and M. G. Bawendi, *J. Phys. Chem. B* **101**, 9463 (1997).
- ²¹R. Xie, U. Kolb, J. Li, T. Basche, and A. Mews, *J. Am. Chem. Soc.* **127**, 7480 (2005).
- ²²D. V. Talapin, I. Mekis, S. Gotzinger, A. Kornowski, O. Benson, and H. Weller, *J. Phys. Chem. B* **108**, 18826 (2004).
- ²³Y. J. Cheng, M. S. Liu, Y. Zhang, Y. H. Niu, F. Huang, J. W. Ka, H. L. Yip, Y. Q. Tian, and A. K.-Y. Jen, *Chem. Mater.* **20**, 413 (2008).
- ²⁴S. A. Empedocles and M. G. Bawendi, *Science* **278**, 2114 (1997).
- ²⁵J. Muller, J. M. Lupton, P. G. Lagoudakis, F. Schindler, R. Koeppe, A. L. Rogach, J. Feldmann, D. V. Talapin, and H. Weller, *Nano Lett.* **5**, 2044 (2005).
- ²⁶E. Rothenberg, M. Kazes, E. Shaviv, and U. Banin, *Nano Lett.* **5**, 1581 (2005).
- ²⁷W. K. Woo, K. T. Shimizu, M. V. Jarosz, R. G. Neuhauser, M. A. Rubner, and M. G. Bawendi, *Adv. Mater. (Weinheim, Ger.)* **14**, 1068 (2002).
- ²⁸H. Huang, A. Dorn, G. P. Nair, V. Bulovic, and M. G. Bawendi, *Nano Lett.* **7**, 3781 (2007).
- ²⁹X. Z. Jiang, S. Liu, M. S. Liu, P. Herguth, A. K.-Y. Jen, H. Fong, and M. Sarikaya, *Adv. Funct. Mater.* **12**, 745 (2002).
- ³⁰C. R. Kagan, C. B. Murray, M. Nirmal, and M. G. Bawendi, *Phys. Rev. Lett.* **76**, 1517 (1996).